

From unconventional insulating behavior towards conventional magnetism in the intermediate-valence compound SmB_6

J. Derr, G. Knebel, D. Braithwaite, B. Salce, and J. Flouquet

Département de la Recherche Fondamentale sur la Matière Condensée, SPSMS, CEA Grenoble, 17 rue des Martyrs, 38054 Grenoble Cedex 9, France

K. Flachbart and S. Gabáni

Centre of Low Temperature Physics, Slovak Academy of Sciences, SK-04401 Košice, Slovakia

N. Shitsevalova

Institute for Problems of Materials Science, UA-252680 Kiev, Ukraine

(Received 21 April 2008; published 16 May 2008)

In intermediate valence compounds, the subtle quantum equilibrium of two microscopic configurations is at the origin of a very rich physics. SmB_6 is a famous example as it displays an intriguing semiconducting behavior at low pressure and a magnetic phase at high pressure. New transport measurements on SmB_6 under hydrostatic conditions show that the two phenomena are intimately linked. The insulating state vanishes just at the pressure ($p=10$ GPa) where homogeneous long range magnetic order appears. A comparison to previous specific heat experiments clearly points out that a magnetic anomaly is observed in resistivity measurements when excellent hydrostatic conditions are realized. The particular sensitivity of SmB_6 to pressure inhomogeneities may reflect the strong anisotropy in the band structure.

DOI: [10.1103/PhysRevB.77.193107](https://doi.org/10.1103/PhysRevB.77.193107)

PACS number(s): 71.27.+a, 75.20.Hr, 75.30.Mb

The interplay between long range magnetic ordering (LRO) and electronic conduction is a central problem in strongly correlated electronic systems. For example, the debate on the localization of the $4f$ electron is an important issue in the description of magnetic quantum criticality of heavy fermion compounds.¹ However, in this class of intermetallic systems, the size of the Fermi surface is mainly given by the ligands, so insulating ground states are rare.²

The beauty of the intermediate valence (IV) compounds SmS and SmB_6 is that the valence mixing between the Sm^{2+} and Sm^{3+} configurations, according to the equilibrium $\text{Sm}^{2+} \rightleftharpoons \text{Sm}^{3+} + 5d$, governs the mode of electronic conduction. However, real band-structure calculations have to take into account all the different electronic orbitals.³⁻⁵ At large atomic distances (a condition realized in SmS at ambient pressure p), the stable configuration is Sm^{2+} and thus SmS is insulating with a large gap Δ .^{2,6} At short atomic distances (high pressure basically above 10 GPa for SmS), the Sm^{3+} limit will be reached. Under pressure, a transition from Sm^{2+} with $J=0$ angular momentum to the Sm^{3+} Kramer's ion with $J=5/2$ and an associated crystal field (either doublet Γ_7 or quartet Γ_8) may occur and LRO must be recovered at high pressure such as in classical Sm^{3+} intermetallic systems. In the intermediate range, the system prefers to end up in a homogeneous IV state. For SmB_6 , this IV state occurs already at ambient pressure.⁷ However, for SmS , the transition from Sm^{2+} to the IV phase appears at low temperature through a first order transition at $p \sim 1$ GPa.⁶ In this low pressure IV phase, the remarkable feature is that both systems end up at low temperature in an insulating phase as if the electronic conducting pushes the system to be renormalized to the divalent phase even though the valence is near $\nu=2.6$ (see Refs. 3-5 and 8 and references therein). These IV systems are characterized by a small gap (Δ) at the Fermi

level. At first glance, the mechanism responsible for the formation of the insulating gap is the hybridization between the $4f$ level and the conduction band.⁹ Despite extensive theoretical analysis such as a Kondo insulator approach,¹⁰ an excitonic view,¹¹ and improvements in the hybridization model,¹² the problem of the origin of the gap is still under debate.

The field has recently been renewed after the discovery of LRO under pressure in SmS and SmB_6 .¹³⁻¹⁶ It was generally agreed that the charge fluctuations linked to the noninteger value of the valence would prevent Ruderman-Kittel-Kasuya-Yosida interactions^{17,18} and LRO could not be established. In the case of SmS , the closure of the gap was found to coincide with the appearance of magnetism.¹⁴ Despite all problems concerning the purity of SmS single crystals, whatever the sample's origin, all experiments agree that the collapse of the gap appears at a pressure of $p_\Delta=2$ GPa (see Ref. 19). On the other hand, the case of SmB_6 looks more complex. The value of the full gap Δ_g determined from transport measurements at ambient pressure is of the order of 2-10 meV depending on the sample quality and of the temperature range of the analysis. Furthermore, there is experimentally a wide variation in the critical pressure p_Δ where the gap vanishes, even for samples with the same value of Δ_g at $p=0$. Respectively, p_Δ varies from 4 to more than 7 GPa.²⁰⁻²⁵ These strongly varying values indicate that pressure hydrostaticity may be very important for SmB_6 . Furthermore, no track of LRO has been reported in previous resistivity experiments. For $p > p_\Delta$ on cooling only, a broad maximum in the resistivity at a temperature T_{max} is observed and not a sharp feature indicating a phase transition. Therefore, we propose in this letter to solve this experimental discrepancy in SmB_6 results by performing transport measurements on the same SmB_6 sample under different hydrostaticity condi-

tions. The energy gap Δ_g can be derived from the activation law of the resistivity for an insulator, $\rho \propto \exp(\Delta_g/2k_B T)$. Under hydrostatic conditions, as for SmS, the closure of the gap appears at the same pressure where a homogeneous LRO occurs.

Single crystals of SmB₆ were prepared by using the floating zone melting technique. The ratio between resistivity at 4.2 and 300 K was nearly 4 orders of magnitude for these crystals. It is worthwhile to mention that such a huge increase in cooling is not observed for SmS inside its low pressure intermediate valent gold phase. Thus, for the same degree of intermediate valence ($v \sim 2.6-2.7$), SmB₆ single crystals can be produced with much higher purity than SmS (see Ref. 14). Specific heat measurements at low temperature²⁴ indicate a linear temperature contribution γT with $\gamma = 12 \text{ mJ mol}^{-1} \text{ K}^{-2}$. The high value of the resistivity at low temperature as well as the small value of γ leads us to rank our sample among the best material studied.²⁰⁻²³ The SmB₆ sample has been cleaved and two pieces of about $200 \times 100 \times 50 \text{ } \mu\text{m}^3$ have been extracted for the high pressure experiments in two different pressure cells. The electrical contacts are made by gold wires that have been spot-welded on the sample. At first, a Bridgman-type cell with tungsten carbide anvils and steatite as pressure medium has been used. Here, the pressure is determined by the superconducting transition of lead. Taking the transition width, the pressure inhomogeneities are at least 10% of the pressure. In Ref. 26, it has been shown that strong uniaxial stress can be induced under these pressure conditions. A second experiment has been performed in a diamond anvil cell (DAC) with argon as a pressure medium. Argon guarantees a very good hydrostaticity of at least up to 10 GPa. The pressure is monitored *in situ* by the fluorescence of ruby spread in the cell, no significant broadening of the fluorescence spectra under high pressure has been observed. The Bridgman cell has been cooled in a classical ⁴He cryostat and pressure has been changed step by step at room temperature. The DAC has been installed in a cryostat where the pressure can be changed *in situ* at low temperature.²⁷ The resistivity has been measured as function of temperature down to 2 K by a four point dc method. The residual resistivity ρ_0 will be the value of ρ at $T=2 \text{ K}$.

The electrical resistivity of SmB₆ is plotted as a function of temperature in Fig. 1 for both experiments. Striking differences appear in the pressure dependence of the resistivity in the two cells. At 4 GPa, the resistivity in the Bridgman cell shows already metallic behavior at low temperatures, whereas only very slight changes are observed in the DAC. The temperature dependence of the resistivity at different pressures in the Bridgman cell is more or less coherent with previous contributions.²⁰⁻²⁴ However, the results obtained in the DAC with better hydrostatic conditions are quite different. Below 8 GPa, the residual resistivity ρ_0 is almost pressure independent. However, ρ_0 loses 4 orders of magnitude in a pressure range of less than 1 to around 10 GPa. Remarkably, above 10 GPa, a sharp decrease in the resistivity occurs below its maximum at T_{max} . As shown in the inset of Fig. 1(b), T_{max} is close to the temperature T_M where at the same pressure $p = 10.6 \text{ GPa} > p_{\Delta}$, a clear phase transition is observed in our microcalorimetric experiment.¹⁶ Nuclear for-

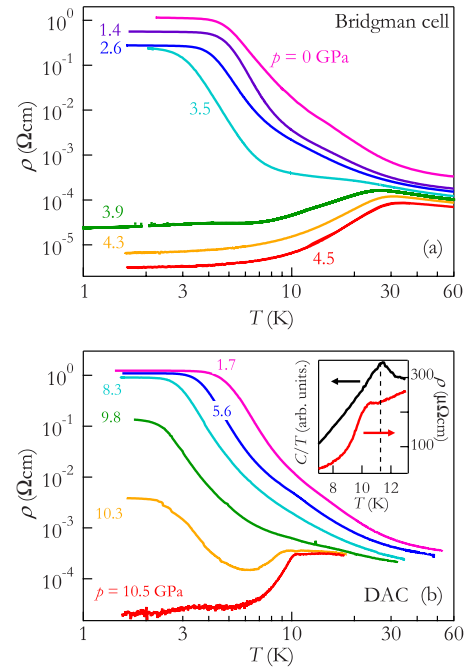


FIG. 1. (Color online) Resistivity (ρ) as a function of temperature (T) for SmB₆ in two different pressure cells, (a) a Bridgman anvil cell, (b) a diamond anvil cell (excellent hydrostaticity). Metallic conduction appears under hydrostatic conditions only above 10 GPa. The inset in (b) shows the magnetic anomaly at $p = 10.6 \text{ GPa}$ by ac calorimetry (black line) and resistivity (red).

ward scattering (NFS) experiments have demonstrated that the phase transition is associated to LRO.¹⁵ The fact that T_M corresponds to a minimum of ρ may mark an antiferromagnetic ground state with zone boundary reconstruction or nesting effects. The observed well defined feature is due to the excellent hydrostaticity established in the cell. In order to verify this result, a second DAC was set up and these findings were confirmed.²⁴ In the following, we will only discuss the results obtained in the DAC.

In order to analyze the insulating properties of SmB₆, the resistivity is plotted in Fig. 2(a) in an Arrhenius representa-

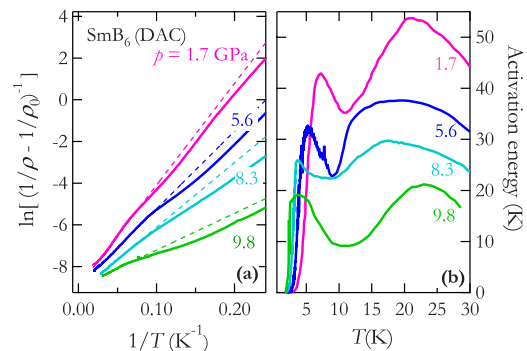


FIG. 2. (Color online) (a) Resistivity of SmB₆ measured in the DAC [Fig. 1(b)] in an Arrhenius representation (solid lines). The dotted lines are a linear fit in the temperature range above 10 K indicating the activated behavior. (b) Temperature dependence of the local activation energy, which is defined as the $d[\ln[(\rho^{-1} - \rho_0^{-1})^{-1}]]/d(1/k_B T)$ (the derivative of the Arrhenius plot).

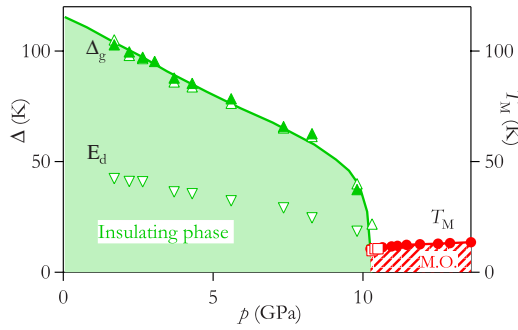


FIG. 3. (Color online) Temperature-pressure phase diagram of SmB_6 . The insulating phase is delimited by the value of the full gap Δ_g [(full triangle up) from the Arrhenius plot, (open triangle up) from the local derivative] and the magnetic ordering temperature T_M is determined from this resistivity measurement (open squares). Previous calorimetry measurement¹⁶ performed in similar pressure conditions are also added to the figure (full circles). Open triangles down give the activation energy of the localized carriers.

tion. Two main contributions to the resistivity of SmB_6 are obvious. The first one is the residual resistivity ρ_0 ($T \ll \Delta_g$), which represents the conduction at very low temperature either by in-gap states or by another channel that is still not clarified.^{12,28,29} The change of ρ_0 is naturally linked to the variation of the valence and thus to the approach of the trivalent limit. The second contribution to ρ is linked to the thermally activated conduction through the gap and can be described by an Arrhenius law, $\rho_{act} \propto \exp(\Delta_g/2k_B T)$ for $T \gtrsim 10$ K. Therefore, the total parallel resistivity is $[\rho_0^{-1} + \rho_{act}^{-1}]^{-1}$ and the gap Δ_g is given in Kelvin by the slope of $\ln[(\rho^{-1} - \rho_0^{-1})^{-1}]$ versus $(1/T)$. In order to estimate Δ_g , we have fitted the Arrhenius curve in its linear part and obtained the pressure dependence of the energy gap (see Fig. 2). However, below 10 K, the electronic conductivity is dominated by localized charge carriers with a lower excitation energy E_d deduced from $\rho \propto \exp(E_d/k_B T)$; see Ref. 30. The two characteristic energy scales of the conductivity can be nicely seen in Fig. 2(b), which shows the temperature dependence of the local activation energy, which is given by $d[\ln[(\rho^{-1} - \rho_0^{-1})^{-1}]]/d(1/k_B T)$ (the derivative of the Arrhenius plot; see also Ref. 23).

Figure 3 shows the temperature-pressure phase diagram obtained by combining this work with previous specific heat measurements.¹⁶ The first observation is that the gap vanishes for the same pressure $p \approx 10$ GPa where magnetism appears, as in the case of SmS .¹⁴ The two techniques (resistivity and specific heat) match very well for the determination of the homogeneous onset of LRO. Nevertheless, the temperature variation of the resistivity at 10.3 GPa clearly indicates that the system is at the same time insulating and LRO (see Fig. 1). As at the critical pressure, both the gaps Δ_g and E_d are finite and T_M is close to 12 K, the transition at p_Δ is first order. Similar effects have recently been observed for SmS in thermal expansion data, which could be fitted by a superposition of a Schottky such as anomaly and a magnetic component for a very small pressure range around p_Δ .³¹ For SmB_6 , a broad specific heat anomaly related to the appearance of a heterogeneous LRO phase is already observed in the pressure range from 8 to 10 GPa.¹⁶

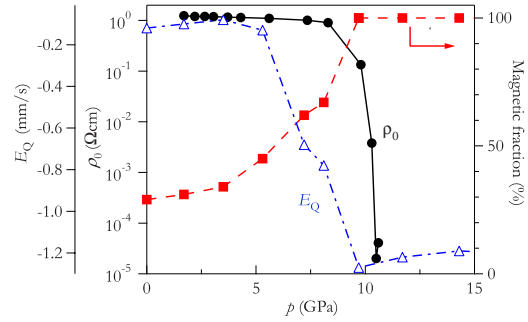


FIG. 4. (Color online) Comparison of the decrease of the residual resistivity (\bullet), the sudden increase of the magnetic volume fraction (\blacksquare), and the average electric quadrupole interaction E_Q at 3 K (Δ) of SmB_6 . The magnetic fraction and E_Q is from nuclear forward scattering (see Ref. 15).

The simultaneous collapse of the insulating state and the onset of LRO is also reinforced by the link between the pressure dependence of ρ_0 , the onset of full homogeneous LRO determined by NFS (Ref. 15) via the restoration of the full magnetic fraction (see Fig. 4) and the establishment of an electric field gradient characteristic of a Γ_8 crystal field ground state. Up until now, no theory tries to correlate the drop of ρ_0 with the homogeneous observation of a unique hyperfine spectrum. NFS experiments underline, however, the establishment of slow spin dynamics of Sm atoms deep inside the insulating phase for both systems, SmS and SmB_6 .

A clear mark of the strong sensitivity of SmB_6 to pressure inhomogeneities is shown by the strong reduction observed in ρ_0 when uniaxial stress σ is applied along (1,1,1) despite the fact that the gap measured by the activation law is almost invariant, whatever the direction of the application of the stress σ .³² The (1,1,1) direction is a privileged axis for the development of correlations and for the softening of the gap. This has been pointed out already by neutron scattering³³ and thermoelectric power measurements.³⁴ In neutron scattering, at $p=0$, a pronounced maximum of the IV excitations at 14 meV occurs along (1,1,1) while almost no intensity occurs for (1,0,0).³³ Furthermore, band-structure calculations³⁻⁵ show the complexity of the electronic structure of SmB_6 , which is linked to the strong hybridization between the Sm 4f electrons and the p electrons of the six boron atoms whatever is the Sm valence. This situation is quite different from SmS . It is striking to remark that in a cubic cage compound such as $\text{PrFe}_4\text{P}_{12}$ with strong hybridization between the 4f and the p electrons the phase diagram was recently found to strongly react to pressure inhomogeneities.³⁵

The measurement of the hyperfine and electric quadrupole interaction by NFS shows that a well defined Γ_8 crystal field ground state is also established at around 10 GPa (see Fig. 4). The simultaneity of the events agree with the idea developed for SmS (Ref. 36) that LRO with an associated metallic state will immediately appear when the crystal field scheme of the trivalent configuration is detected even if the valence is far less than 3. In SmS , this has been detected in recent x-ray experiments ($v=2.8$ at $p_\Delta=2$ GPa) (Ref. 38). Below p_Δ , it is also worthwhile to mention that it was predicted³⁷ that a Γ_8 ground state will favor the gap opening while a Γ_7 choice will preclude such a possibility, in agreement with the

experiment.¹⁵ In the IV system YbInCu₄ where the valence mixing also occurs between the 2⁺ and 3⁺ configurations, LRO emerges when the crystal field is observable;³⁹ here again a pressure window exists with coexisting paramagnetic and LRO phases.

To summarize, these transport measurements unambiguously demonstrate the coincidence between the collapse of the insulating gap and the onset of LRO in SmB₆. An important feature is that despite differences in the crystal and elec-

tronic structure as well as in the hybridization strength between SmB₆ and SmS, the transition at p_{Δ} is governed by the same phenomenon. Furthermore, their phase transition at p_{Δ} adds another example of a first order transition to the list of heavy fermion phase transition at low temperatures.

The work was partially supported by the Slovak agencies VEGA-7054, APVV-034607 and the French ANR within the ICENET and ECCE projects.

-
- ¹S. J. Yamamoto and Q. Si, Phys. Rev. Lett. **99**, 016401 (2007).
²P. Wachter, *Handbook on the Physics and Chemistry of Rare Earth*, edited by K. A. Gschneidner and L. Eyring (Elsevier Science, Amsterdam, 1993), Vol. 19.
³A. Yanase and H. Harima, Prog. Theor. Phys. Suppl. **108**, 19 (1992).
⁴V. N. Antonov, B. N. Harmon, and A. N. Yaresko, Phys. Rev. B **66**, 165208 (2002).
⁵V. N. Antonov, B. N. Harmon, and A. N. Yaresko, Phys. Rev. B **66**, 165209 (2002).
⁶A. Jayaraman, V. Narayanamurti, E. Bucher, and R. G. Maines, Phys. Rev. Lett. **25**, 1430 (1970).
⁷J. C. Nickerson, R. M. White, K. N. Lee, R. Bachmann, T. H. Geballe, and G. W. Hull, Jr., Phys. Rev. B **3**, 2030 (1971).
⁸L. Degiorgi, Rev. Mod. Phys. **71**, 687 (1999).
⁹B. Coqblin and A. Blandin, Adv. Phys. **17**, 281 (1968).
¹⁰T. Kasuya, Europhys. Lett. **26**, 277 (1994).
¹¹K. A. Kikoin and A. S. Mischenko, J. Phys.: Condens. Matter **7**, 307 (1995).
¹²P. S. Riseborough, Phys. Rev. B **68**, 235213 (2003).
¹³A. Barla, J. P. Sanchez, Y. Haga, G. Lapertot, B. P. Doyle, O. Leupold, R. Ruffer, M. M. Abd-Elmeguid, R. Lengsdorf, and J. Flouquet, Phys. Rev. Lett. **92**, 066401 (2004).
¹⁴Y. Haga, J. Derr, A. Barla, B. Salce, G. Lapertot, I. Sheikin, K. Matsubayashi, N. K. Sato, and J. Flouquet, Phys. Rev. B **70**, 220406(R) (2004).
¹⁵A. Barla, J. Derr, J. P. Sanchez, B. Salce, G. Lapertot, B. P. Doyle, R. Ruffer, R. Lengsdorf, M. M. Abd-Elmeguid, and J. Flouquet, Phys. Rev. Lett. **94**, 166401 (2005).
¹⁶J. Derr, G. Knebel, G. Lapertot, B. Salce, M.-A. Measson, and J. Flouquet, J. Phys.: Condens. Matter **18**, 2089 (2006).
¹⁷T. V. Ramakrishnan and K. Sur, Phys. Rev. B **26**, 1798 (1982).
¹⁸C. M. Varma, Physica B (Amsterdam) **378-380**, 17 (2006).
¹⁹F. Lapierre, M. Ribault, J. Flouquet, and F. Holtzberg, J. Magn. Magn. Mater. **31**, 443 (1983).
²⁰J. Beille, M. B. Maple, J. Wittig, Z. Fisk, and L. E. DeLong, Phys. Rev. B **28**, 7397 (1983).
²¹V. V. Moshchalkov, I. V. Berman, N. B. Brandt, S. N. Pashkevich, E. V. Bogdanov, E. S. Konovalova, and M. V. Semenov, J. Magn. Magn. Mater. **47-48**, 289 (1985).
²²J. C. Cooley, M. C. Aronson, Z. Fisk, and P. C. Canfield, Phys. Rev. Lett. **74**, 1629 (1995).
²³S. Gabani, E. Bauer, S. Berger, K. Flachbart, Y. Paderno, C. Paul, V. Pavlik, and N. Shitsevalova, Phys. Rev. B **67**, 172406 (2003).
²⁴J. Derr, Ph.D. thesis, Université Joseph Fourier, 2006.
²⁵M. Chiao (private communication, 2006).
²⁶A. Demuer, A. T. Holmes, and D. Jaccard, J. Phys.: Condens. Matter **14**, L529 (2002).
²⁷B. Salce, J. Thomasson, A. Demuer, J. J. Blanchard, J. M. Martinod, L. Devoille, and A. Guillaume, Rev. Sci. Instrum. **71**, 2461 (2000).
²⁸S. Curnoe and K. A. Kikoin, Phys. Rev. B **61**, 15714 (2000).
²⁹S. Gabáni, K. Flachbart, E. Konovalova, M. Orendac, Y. Paderno, V. Pavlik, and J. Sebek, Solid State Commun. **117**, 641 (2001).
³⁰B. Gorshunov, N. Sluchanko, A. Volkov, M. Dressel, G. Knebel, A. Loidl, and S. Kunii, Phys. Rev. B **59**, 1808 (1999).
³¹K. Imura, K. Matsubayashi, H. S. Suzuki, T. Nishioka, N. Mori, and N. K. Sato, Physica B (Amsterdam) **378-380**, 728 (2006).
³²J. Derr, G. Knebel, G. Lapertot, B. Salce, S. Kunii, and J. Flouquet, J. Magn. Magn. Mater. **310**, 560 (2007).
³³P. A. Alekseev, J.-M. Mignot, J. Rossat-Mignod, V. N. Lazukov, I. P. Sadikov, E. S. Konovalova, and Yu. B. Paderno, J. Phys.: Condens. Matter **7**, 289 (1995).
³⁴N. E. Sluchanko, V. V. Glushkov, S. V. Demishev, A. A. Pronin, A. A. Volkov, M. V. Kondrin, A. K. Savchenko, and S. Kunii, Phys. Rev. B **64**, 153103 (2001).
³⁵H. Hidaka, N. Wada, H. Kotegawa, T. Kobayashi, D. Kikuchi, H. Sato, and H. Sugawara, J. Magn. Magn. Mater. **310**, e228 (2007).
³⁶J. Flouquet, A. Barla, R. Boursier, J. Derr, and G. Knebel, J. Phys. Soc. Jpn. **74**, 178 (2005).
³⁷K. Hanzawa, J. Phys. Soc. Jpn. **67**, 3151 (1998).
³⁸E. Annese, A. Barla, C. Dallera, G. Lapertot, J. P. Sanchez, and G. Vanko, Phys. Rev. B **73** 140409(R) (2006).
³⁹T. Park, V. A. Sidorov, J. L. Sarrao, and J. D. Thompson, Phys. Rev. Lett. **96**, 046405 (2006).